Unsteady Loading on Airfoil Due to Vortices Released Intermittently from Its Surface

Chuen-Yen Chow*and Chyn-Shan Chiu†
University of Colorado, Boulder, Colorado

An unsteady flow analysis is made of the flow past a symmetric airfoil with identical vortices released intermittently from its upper surface. The vortex train is used to simulate the flow observed in the laboratory, which was perturbed by an oscillating spoiler or a rotating cam embedded in the airfoil surface. Based on numerical computations, the airfoil lift generally increases oscillationally with time and seems to approach an asymptotic value as time increases indefinitely. The asymptotic lift is enhanced with increasing frequency and is only slightly influenced by changing the vortex-releasing position along the chord. The behavior of the drag is similar to that of the lift, but its magnitude is two orders smaller. Our study also indicates that it is more efficient to implement the vortex-augmented unsteady lift at higher angles of attack of the airfoil.

Nomenclature

a	= radius of circle that maps into an airfoil
c	= airfoil chord
C_D, C_L, C_P	= drag, lift, and pressure coefficients, respectively
D	= drag
k_j	= circulation of jth vortex
K	= reduced frequency
L	= lift
m	= total number of discrete vortices in flow
$\boldsymbol{R}$	= position vector of a vortex
t	= time
T	= period of oscillation
u, v	= horizontal and vertical velocity components, respectively
V	= freestream speed
$\boldsymbol{V}$	= velocity vector
w	= complex potential
x, y	= horizontal and vertical coordinates, respectively, in physical plane
z	= $x+iy$, complex position in physical plane
α	= angle of attack
Γ	= initial circulation about airfoil
ζ	= $\xi+i\eta$, complex position in circle plane
ξ, η	= horizontal and vertical coordinates, respectively, in circle plane
ρ	= fluid density
ω	= angular frequency of oscillation

Introduction

EXPERIMENTS have been conducted to study the flow past an airfoil, which was perturbed by an oscillating fence-type spoiler protruding from the upper surface, like the device used by Francis et al.,[1] or by a rotating cam-shaped rotor adopted by Viets et al.[2] In these experiments, organized vortex structures were observed to form periodically behind the perturbing mechanism and to be carried into the wake by the local streaming fluid motion.

When moving along the airfoil surface, this train of vortices not only makes the flow unsteady but also may cause significant changes in airfoil performance. While empirical data are not yet available for comparison, we present here a theoretical analysis for computing the unsteady lift, drag, and pressure distribution on the airfoil when vortices are released intermittently from its upper surface.

Although vortices observed in the laboratory are most likely formed from rolling up of vortex sheets resulting from boundary-layer separation at the sharp tip of the spoiler or rotor as sketched in Fig. 1, they are treated as discrete potentail vortices in our formulation, based on an inviscid incompressible flow analysis. The symmetric airfoil configuration adopted in our computation is generated from a circle through a Joukowski transformation, and the effect of the oscillating spoiler or rotating cam is simulated by the intermittent appearance of discrete vortices of the same strength at a given location above the airfoil. In an unsteady flow about the airfoil, a vortex sheet is expected to shed continuously from the sharp trailing edge. Strengths of the discretized wake vortices and the instantaneous circulation about the airfoil are determined from requirements that the resultant flow be tangent to the airfoil surface, the Kutta condition be satisfied at all times, and the total circulation in the entire flowfield be kept at the initial value. The complex potential for the physical flow about the airfoil is obtained using conformal mapping techniques, and the unsteady flow problem is solved step by step by marching with a small time increment.

Computational Procedure

The theoretical analysis and computational procedure for obtaining a solution are briefly outlined here. Details of this analysis can be found in Ref. 3. All variables shown in the following formulation are made dimensionless using the freestream speed V ahead of the airfoil as the reference speed, approximately half of the chord, $c/2$, as the reference length, and the time required for the freestream to travel one reference length as the reference time. Let ω be the angular frequency in rad/s of the oscillatory motion of the vortex-generating mechanism. The reduced frequency K is defined as $\omega c/2V$ so that the dimensionless period T of the oscillation is $2\pi/K$.

As shown in Fig. 2, the transformation

$$z=\frac{1}{2}\left(\zeta'+\frac{1}{\zeta'}\right) \tag{1}$$

Received April 11, 1985; revision received June 10, 1986.

*Professor, Department of Aerospace Engineering Sciences. Associate Fellow AIAA.

†Graduate Student, Department of Aerospace Engineering Sciences. Presently, Deputy Chief, Aerodynamics Branch, Aeronautical Research Laboratory, Taichung, Taiwan.

maps a circle of radius a (>1) in the $\zeta'(=\xi'+i\eta')$ plane, centered at $\zeta'=1-a$, into a symmetric Joukowski airfoil in the physical $z(=x+iy)$ plane, whose chord is slightly longer than 2. A freestream velocity of a magnitude of one-half and at an angle of attack α is mapped without changing its orientation into a uniform stream of unit speed in the physical plane. For convenience of formulation, a $\zeta(=\xi+i\eta)$ plane is introduced in Fig. 2, whose origin coincides with the center of the circle. The relation

$$\zeta=\zeta'+a-1 \tag{2}$$

holds for coordinate transformation between ζ and ζ' planes.

A discrete vortex of circulation k_j at a position z_j outside the airfoil is transformed according to Eq. (1) into a vortex of the same strength at ζ_j outside the circle. To satisfy the boundary condition that the flow be tangent to the circle and to fulfill the requirement that the total circulation be conserved, an image vortex of strength $-k_j$ and another vortex of strength k_j are added at $a^2/\bar{\zeta}_j$ and the center of the circle, respectively. For each of the discrete vortices in the physical plane, be it the vortex generated by a spoiler or a vortex shed in the wake, a set of three vortices is placed in the transformed plane-following the procedure just described. Suppose the initial steady-state circulation about the airfoil is Γ, which is determined by the airfoil angle of attack α. After vortices have been generated by a perturbing mechanism, the total circulation in the entire flow must be kept at its initial value according to the inviscid theory. In other words, no matter how many vortices are present in the flow, the total strength of all vortices situated at the center of the circle in the transformed plane must be Γ at all times. Thus when a vortex appears in the flow, it is sufficient to represent it by a vortex pair across the circle as shown in Fig. 2. The instantaneous circulation around the airfoil is therefore given by

$$\Gamma-\sum_{j=1}^{m} k_j$$

in which m represents the total number of discrete vortices in the flow at that instant.

Properties of the physical flow can be derived from the flow in the transformed plane, whose complex potential at any point ζ outside the circle is

$$w=\frac{1}{2}e^{-i\alpha}\left(\zeta+\frac{a^2}{\zeta}e^{i2\alpha}\right)+\frac{i\Gamma}{2\pi}\log\zeta + \sum_{j=1}^{m}\frac{ik_j}{2\pi}[\log(\zeta-\zeta_j)-\log(\zeta-a^2/\bar{\zeta}_j)] \tag{3}$$

Differentiation of Eq. (3) gives the complex velocity

$$u-iv=\frac{dw}{dz}=\frac{dw}{d\zeta}\Big/\frac{dz}{d\zeta} \tag{4}$$

in which

$$\frac{dw}{d\zeta}=\frac{1}{2}e^{-i\alpha}\left(1-\frac{a^2}{\zeta^2}e^{i2\alpha}\right)+\frac{i\Gamma}{2\pi\zeta} + \sum_{j=1}^{m}\frac{ik_j}{2\pi}\left(\frac{1}{\zeta-\zeta_j}-\frac{1}{\zeta-a^2/\bar{\zeta}_j}\right) \tag{5}$$

$$\frac{dz}{d\zeta}=\frac{\zeta'^2-1}{2\zeta'^2} \tag{6}$$

This expression holds at any point in the physical flow except at the trailing edge of the airfoil and the center of a free vortex.

In the unsteady flowfield, a wake vortex is shed at any instant of time. Let this be the mth vortex whose position is ζ_m in the transformed plane. Its circulation k_m, determined by satisfying the Kutta condition that $\zeta=a$ be a stagnation point, has the expression

$$k_m=\left[2\pi a\sin\alpha-\Gamma-\sum_{j=1}^{m-1}k_j\frac{a^2-\zeta_j\bar{\zeta}_j}{(a-\zeta_j)(a-\bar{\zeta}_j)}\right] \div\frac{a^2-\zeta_m\bar{\zeta}_m}{(a-\zeta_m)(a-\bar{\zeta}_m)} \tag{7}$$

This vortex will later move at the local fluid velocity without changing its circulation.

For numerical computations, we choose $a=1.15$ to obtain a 17% thick symmetric airfoil. The strength of vortices generated by a perturbing device is determined by the size of the device, frequency of oscillation, Reynolds number, and other factors. It can be measured according to a method described by Keesee et al.[4] However, because of insufficient empirical data corresponding to our concerned conditions, we arbitrarily pick a circulation value of 0.5 for all the cases we have examined. This dimensionless strength represents a circulation which, when applied around an airfoil, would produce a lift coefficient of 0.5. For a given angle of attack and prescribed vortex-releasing chordwise position and period, the procedure for numerical computation is outlined as follows.

1) At time $t=0$, the first vortex of circulation $k_1=0.5$ is released at a fixed position z_1 above the airfoil. Instantaneously a wake vortex is shed in order to make the flow smooth

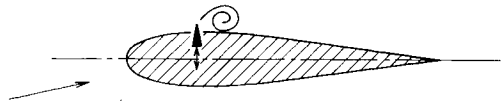

Fig. 1 Vortex generated behind an oscillating spoiler.

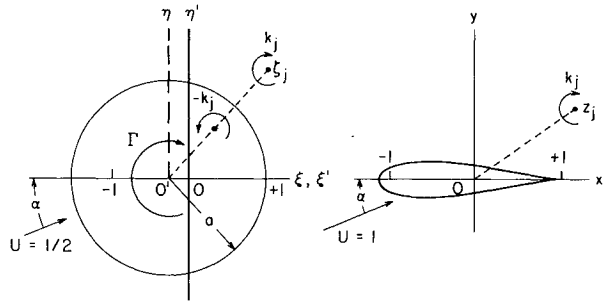

Fig. 2 Mapping between the physical and transformed planes.

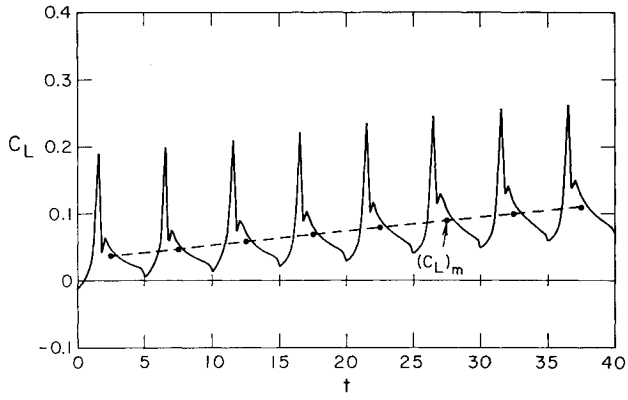

Fig. 3 Initial variation of lift coefficient for $\alpha=0$ deg and $T=5$. Circulation of vortices released at the midchord position is 0.5.

at the trailing edge. We assume that the position of the shed vortex in the transformed plane is at $\zeta_2 = a + 0.1$, so that a short distance is provided behind the airfoil trailing edge to accommodate its viscous core. The circulation k_2 of the first wake vortex is then computed from Eq. (7) with $m = 2$.

2) Complex velocities of all discrete vortices in the physical plane are computed using a general formula for the nth vortex at z_n, derived after taking a proper limit:

$$(u-iv)_{z_n} = \left(\frac{dw}{dz} - \frac{ik_n}{2\pi}\frac{1}{z-z_n}\right)_{\zeta=\zeta_n}$$
$$= \frac{\zeta'^2_n}{\zeta'^2_n - 1}\left[e^{-i\alpha} - \left(\frac{a}{\zeta_n}\right)^2 e^{i\alpha} + \frac{i\Gamma}{\pi\zeta_n} + \sum_{j\neq n}^{m}\frac{ik_j}{\pi}\frac{1}{\zeta_n - \zeta_j} - \sum_{j=1}^{m}\frac{ik_j}{\pi}\frac{1}{\zeta_n - a^2/\bar{\zeta}_j}\right] - \frac{ik_n\zeta'_n}{\pi(\zeta'^2_n - 1)^2} \tag{8}$$

Instantaneous lift L and drag D on the airfoil are computed based on the Blasius theorem for unsteady flow:

$$D + iL = i\rho\Gamma - i\rho e^{-i\alpha}\sum_{j=1}^{m} k_j (u+iv)_{z_j}\frac{\zeta'^2_j}{\zeta'^2_j - 1} - i\rho e^{-i\alpha}\sum_{j=1}^{m} k_j (u-iv)_{z_j}\left(\frac{a}{\bar{\zeta}_j}\right)^2\frac{\bar{\zeta}'^2_j}{\bar{\zeta}'^2_j - 1} \tag{9}$$

Pressure distribution around the airfoil can be determined by computing pressure coefficient from the unsteady Bernoulli's equation:

$$C_p = 1 - \left|\frac{dw}{dz}\right|^2 - 2\frac{\partial}{\partial t}\left[\text{Real}\sum_{j=1}^{m}\frac{ik_j}{2\pi}\log\frac{\zeta-\zeta_j}{\zeta - a^2/\bar{\zeta}_j}\right] \tag{10}$$

3) Time is advanced by an increment Δt, which is chosen as $T/20$ so that one cycle of oscillation is completed in 20 time steps. The new position $\boldsymbol{R}(t+\Delta t)$ of a vortex, whose previous position vector $\boldsymbol{R}(t)$, is calculated using a two-step predictor-corrector procedure.

$$\boldsymbol{R}_p = \boldsymbol{R}(t) + \Delta t \boldsymbol{V}[\boldsymbol{R}(t)] \tag{11}$$

$$\boldsymbol{R}(t+\Delta t) = \boldsymbol{R}(t) + \Delta t\{\boldsymbol{V}[\boldsymbol{R}(t)] + \boldsymbol{V}(\boldsymbol{R}_p)\}/2 \tag{12}$$

where the velocity vectors are those constructed from the complex-velocity expression [Eq. (8)].

4) At the end of that time increment, a new vortex is shed in the wake. Instead of assuming its location as in the case of the first shed vortex, we place it on the x axis at a distance $u_{T.E.}\Delta t$ downstream from the trailing edge, where the horizontal flow speed at the trailing edge is found to be

$$u_{T.E.} = \frac{\cos\alpha}{a} - \text{Real}\left\{\sum_{j=1}^{m}\frac{ik_j}{2\pi}\left[\frac{1}{(a-\zeta_j)^2} - \frac{1}{(a-a^2/\bar{\zeta}_j)^2}\right]\right\} \tag{13}$$

With the position known, the circulation of this shed vortex is computed using Eq. (7).

Numerical computations described in steps 2-4 are then repeated until a desired time level is reached. The number of wake vortices is increased by one at the end of each iteration. The tip of the wake vortex sheet rolls into a spiral, which becomes tighter and tighter as time progresses. When distances among vortices become too small, inaccurate results in the form of scattered vortices in the wake are expected. To eliminate this chaotic motion of the wake vortices, we adopt Moore's method[5] by using a concentrated vortex to represent the tightly rolled portion of a vortex sheet. More specifically, when the total number of wake vortices exceeds 20 in the computation, the first two vortices at the tip of the vortex sheet are combined into one situated at their centroid position, whose circulation is the sum of the two individual strengths.

A procedure different from that described in step 4 was used by Duffy et al.[6] to determine the location of the vortex shed instantaneously by an airfoil in oscillatory motion. They assumed that, in a short time period Δt, a straight vortex sheet of approximately constant strength is shed at the trailing edge into the wake. This wake vortex segment is replaced by a concentrated vortex whose position is determined by requiring that its induced velocity at the 3/4 c point on the airfoil be the same as that induced by the vortex segment. When this procedure was tested in the cases shown in the present work on a stationary airfoil, no appreciable differences were found in aerodynamic computations. However, when these two different procedures were used in our other studies to calculate the location of the first vortex shed by an oscillating airfoil, significant discrepanies were displayed in the results. In the case of an airfoil in unsteady motions, the procedure described in Ref. 6 would be more accurate.

Results

For the 17% thick symmetric airfoil, computations have been made by varying the angle of attack, the chordwise posi-

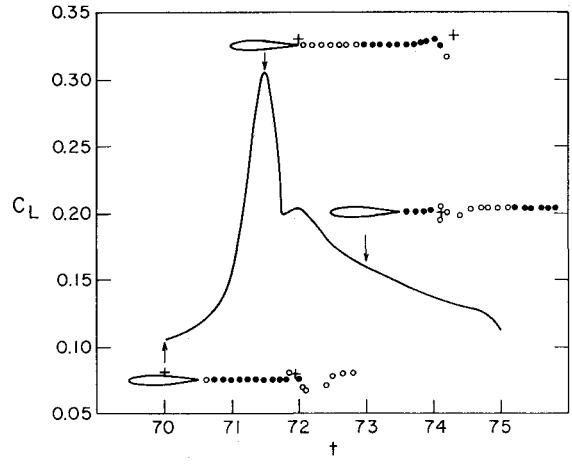

Fig. 4 Variation of lift coefficient and vortical configurations in a representative cycle of spoiler oscillation for $\alpha = 0$ deg and $T = 5$. A cross represents a vortex released from the airfoil surface. The solid and open circles show the positions of wake vortices of clockwise and counterclockwise circulations, respectively.

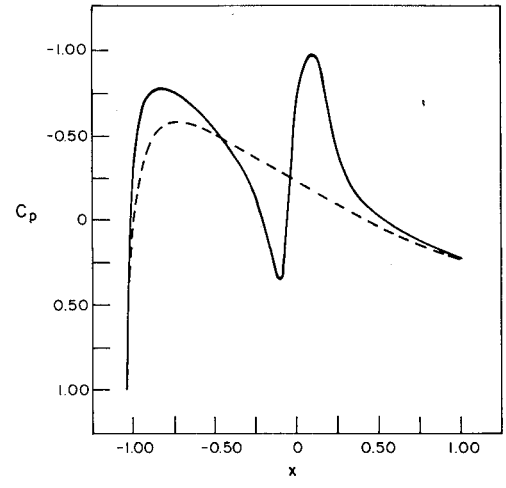

Fig. 5 Distribution of pressure coefficient on the upper surface (solid line) and lower surface (dashed line) of the airfoil shown in Fig. 4 at $t = 0$.

tion of the released vortices, and the period at which they are released.

At zero angle of attack and when vortices of circulation 0.5 are released with a period $T=5$ at a height of 0.1 above the upper surface at $x=0$ near the midchord position, the behavior of the lift coefficient at the early stage is plotted in Fig. 3. The sudden release of a vortex causes a negative lift on the airfoil. Lift increases with time in an oscillatory manner; the mean lift coefficient $(C_L)_m$, averaged within each oscillation, gradually approaches an asymptotic value after more than 50 vortices have been released. The variation of lift in one cycle has a shape almost identical to that in any other cycle, except that the entire curve is shifted upward after each period.

A representative lift curve within one cycle, for $70 \le t \le 75$, is blown up and plotted in Fig. 4. At the beginning of that cycle, when a vortex is just released at the upper surface, lift has the lowest value. At this instant the vortex released in the previous cycle is in the wake at a distance of about four half-chord lengths from the newly released vortex, as shown in the leftmost of the three airfoils in Fig. 4. The shape of the wake vortex sheet is displayed by a group of discretized vortices. At this time the circulation of the vortex shedding from the trailing edge starts to change direction from clockwise to counterclockwise. Lift increases rapidly as the released vortex moves along the airfoil surface; it reaches a maximum when the vortex is about to leave the trailing edge, as sketched in the middle insertion. Afterward, lift drops and vortices of clockwise circulation are shed in the wake until the next vortex is released from the upper surface. The strengths of the wake vortices are at least one order smaller than that of the released vortices.

Three pressure distributions around the airfoil, corresponding respectively to the three different positions of the released vortex sketched in Fig. 4, are plotted for comparison. Figure 5 shows that on the upper surface of the airfoil, there is a low-pressure region below the vortex that has just been released behind the midchord at $t=70$. The higher-pressure region ahead of the vortex causes a decrease in the area enclosed by the pressure curve, resulting in a small net lift on the airfoil. At $t=71.5$, when the vortex has passed the trailing edge, the low-pressure region below the vortex disappears from the surface pressure plotted in Fig. 6. The high pressure ahead of the vortex has a small negative effect in the trailing-edge area, so that the lift at this instant is the highest. At $t=73$, the vortex is at a distance of more than half the chord from the trailing edge; it still has a significant influence on the airfoil, as shown in Fig. 7, giving a positive lift to the airfoil at zero angle of attack.

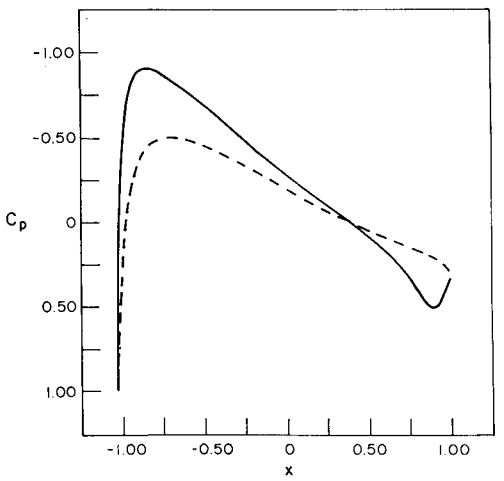

Fig. 6 Distribution of pressure coefficient on the upper surface (solid line) and lower surface (dashed line) of the airfoil shown in Fig. 4 at $t=71.5$.

If the dimensionless period of oscillation is shortened to 1 while keeping all other parameters the same as before, that is, if the vortex-generating frequency is increased five times, lift still increases oscillationally, as shown, in Fig. 8, but parts of the lift remain negative in the first 10 cycles. The lift variation in the 19th cycle is plotted in Fig. 9. The inserted vortex configurations show shorter distances between neighboring released vortices and stronger interactions between these vortices and the wake vortex sheet. It is interesting to note that all wake vortices have counterclockwise circulations. Within that period, lift climbs to a maximum and then drops to a minimum, with both changes occurring when a released vortex leaves the trailing edge.

The variation of mean lift coefficient with time is plotted in Fig. 10 for different values of T. Solid lines represent results for an arrangement in which vortices are released near the midchord location. The plot reveals that for a shorter T, when vortices are released at a higher frequency, a higher average lift can be generated on the airfoil. Each of the higher T curves seems to approach an asymptotic value that increases with increasing frequency. The curves for lower values of T seem to have the same behavior, but a tremendous amount of computer time is needed to find their asymptotic lift values. For example, to reach $t=200$ for the $T=2$ curve, the CPU time is 2700 s on a Cyber 170-720 computer. No attempt has been made to extend the computation beyond that time. However, it should be pointed out that for T equals 2 or 1, the mean lift

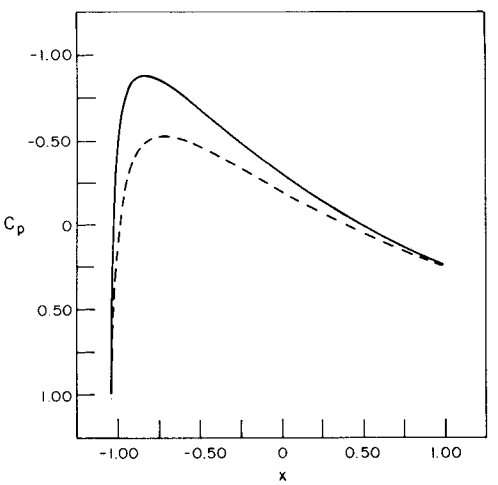

Fig. 7 Distribution of pressure coefficient on the upper surface (solid line) and lower surface (dashed line) of the airfoil shown in Fig. 4 at $t=73$.

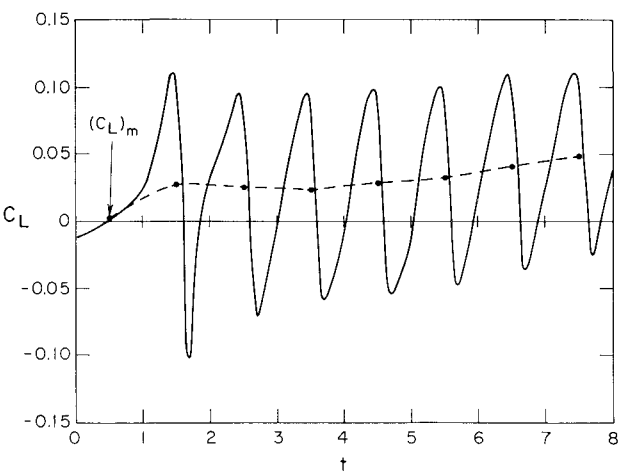

Fig. 8 Initial variation of lift coefficient for $\alpha=0$ deg and $T=1$. Circulation of vortices released at the midchord position is 0.5.

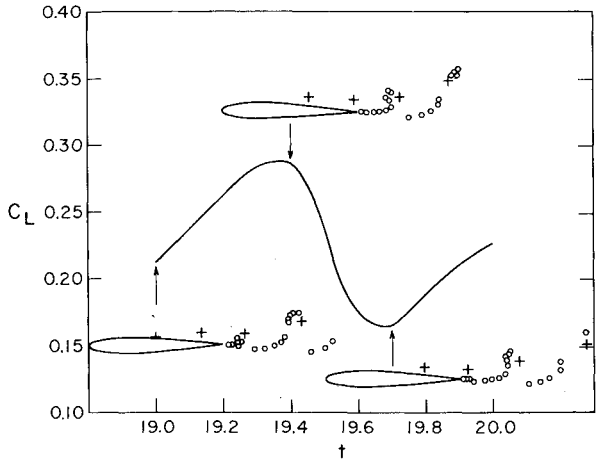

Fig. 9 Variation of lift coefficient and vortical configurations in a representative cycle of spoiler oscillation for $\alpha = 0$ deg and $T = 1$. Meaning of crosses and open circles can be found under Fig. 4.

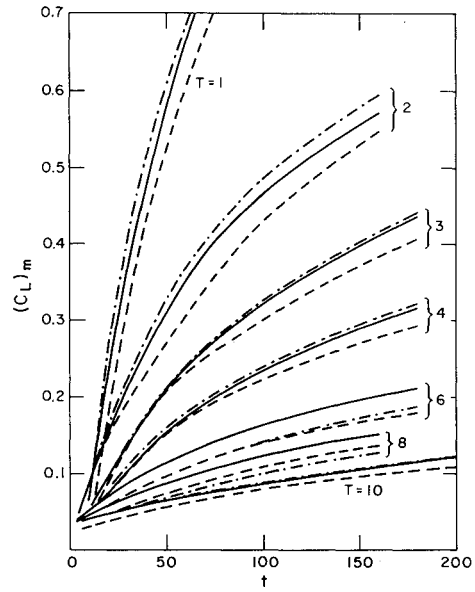

Fig. 10 Variation of mean lift coefficient with time for different periods. Airfoil angle of attack is zero and circulation of released vortices is 0.5. Results shown are for vortices released at midchord (solid lines), quarter-chord (dashed lines), and 3/4-chord (dashed-dotted lines) positions.

coefficient becomes greater than 0.5 within the time range of Fig. 10, which is the static lift coefficient if the circulation of a released vortex is applied around the airfoil.

The dashed and the dashed-dotted lines in Fig. 10 are used to represent results obtained when the vortex-generating mechanism is near the 1/4-chord and 3/4-chord positions, respectively. In these two cases, vortices are still released at the same initial height of 0.1 above the local airfoil surface. The influence of changing chordwise position on lift is not too strong as revealed in the figure. Generally speaking, releasing vortices at the 1/4-chord position causes a decrease in average lift, whereas shifting it rearward to the 3/4-chord position does the opposite for $T = 10$ and $T \leq 5$.

Plotted in Figs. 11 and 12 is the initial behavior of drag coefficient for $T = 5$ and 1, respectively. The general pattern of drag variation is similar to that of the lift, but the magnitude is two orders smaller. The mean drag coefficient $(C_D)_m$, averaged over one period, approaches negative and positive asymptotic values, respectively, for $T = 5$ and 1.

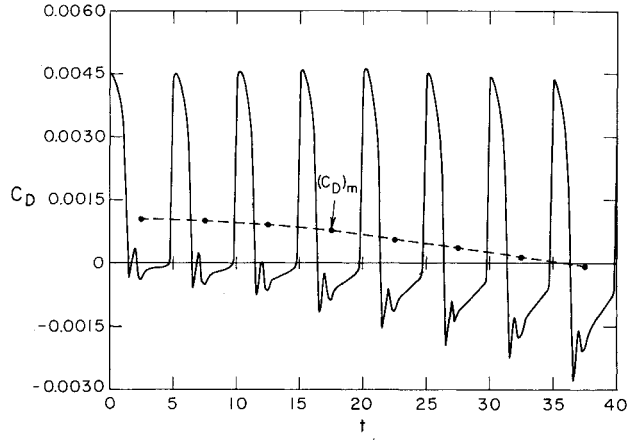

Fig. 11 Initial variation of drag coefficient for $\alpha = 0$ deg and $T = 5$. Circulation of vortices released at the midchord position is 0.5.

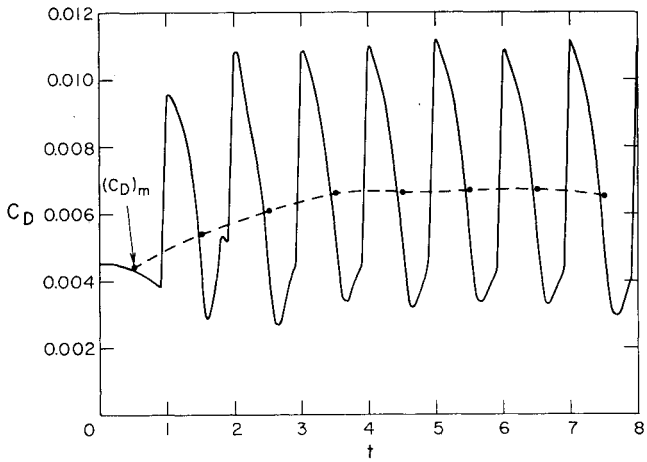

Fig. 12 Initial variation of drag coefficient for $\alpha = 0$ deg and $T = 1$. Circulation of vortices released at the midchord position is 0.5.

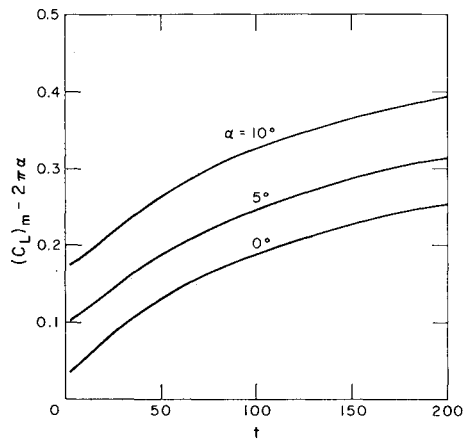

Fig. 13 Effect of angle of attack on time variation of mean incremental lift coefficient for the case when vortices are released at midchord position at period $T = 5$.

The effect of changing airfoil angle of attack on mean lift coefficient is examined. A representative result, obtained for the case in which vortices are released at the midchord location at $T = 5$, is shown in Fig. 13. Plotted against time in this figure is the mean incremental lift coefficient, defined as $(C_L)_m - 2\pi\alpha$. A comparison of the curves for $\alpha = 0$, 5, and 10 deg indicates that the vortex-augmented unsteady lift increases with increasing angle of attack.

Discussion

Our study shows that lift is significantly affected by the vortices released intermittently above an airfoil. According to the analysis for an inviscid flow, an extra unsteady lift can be generated on a wing utilizing a properly designed vortex-triggering device installed on its upper surface. Despite the negligibly small magnitude as predicted by the inviscid theory, the drag can be expected to be substantial in reality when vortices are generated by moving a spoiler into and out of the airfoil surface.

The strength of the released vortices is arbitrarily assigned in the present analysis. Actually, it should be determined more realistically from empirical data or from viscous flow computations. The authors are taking the latter approach in an attempt to solve the problem of an unsteady viscous flow past an oscillating spoiler.

Acknowledgment

This work was supported by the U.S. Air Force Office of Scientific Research under Grant 81-0037.

References

[1] Francis, M.S., Keesee, J.E., Lang, J.D., Sparks, G.W., and Sisson, G.E., "Aerodynamic Characteristics of an Unsteady Separated Flow," *AIAA Journal,* Vol. 17, Dec. 1979, pp. 1332-1339.

[2] Viets, H., Piatt, M., and Ball, M., "Unsteady Wing Boundary Layer Energization," AIAA Paper 79-1631, Aug. 1979.

[3] Chow, C.-Y. and Huang, M.-K., "Unsteady Flows About a Joukowski Airfoil in the Presence of Moving Vortices," AIAA Paper 83-0129, Jan. 1983.

[4] Keesee, J.E., Francis, M.S., and Lang, J.D., "Technique for Vorticity Measurement in Unsteady Flow," *AIAA Journal,* Vol. 17, April 1979, pp. 387-393.

[5] Moore, D.W., "A Numerical Study of the Roll-Up of a Finite Vortex Sheet," *Journal of Fluid Mechanics,* Vol. 63, 1974, pp. 225-235.

[6] Duffy, R.E., Czajkowski, E., and Jaran, C., "Finite Element Approximation to Theodorsen's Solution for Nonsteady Aerodynamics of an Airfoil Section," AIAA Paper 84-1640, June 1984.